Steady-state kinetics and inhibition of anaerobically purified human homogentisate 1,2-dioxygenase

Edwin J. A. VELDHUIZEN*[1,2], Frédéric H. VAILLANCOURT†[1,3], Cheryl J. WHITING*, Marvin M.-Y. HSIAO†, Geneviève GINGRAS‡, Yufang XIAO‡, Robert M. TANGUAY§, John BOUKOUVALAS‡ and Lindsay D. ELTIS*†[4]

*Department of Microbiology and Immunology, University of British Columbia, 300-6174 University Blvd, Vancouver, BC, Canada V6T 1Z3, †Department of Biochemistry and Molecular Biology, University of British Columbia, Vancouver, BC, Canada V6T 1Z3, ‡Department of Chemistry, Université Laval, Quebec City, QC, Canada G1K 7P4, and §Laboratoire de Génétique Cellulaire et Développementale, Département de Médecine, Pavillon Marchand, Université Laval, Quebec City, QC, Canada G1K 7P4

HGO (homogentisate 1,2-dioxygenase; EC 1.13.11.5) catalyses the O_2-dependent cleavage of HGA (homogentisate) to maleylacetoacetate in the catabolism of tyrosine. Anaerobic purification of heterologously expressed Fe(II)-containing human HGO yielded an enzyme preparation with a specific activity of 28.3 ± 0.6 μmol · min^{-1} · mg^{-1} (20 mM Mes, 80 mM NaCl, pH 6.2, 25 °C), which is almost twice that of the most active preparation described to date. Moreover, the addition of reducing agents or other additives did not increase the specific activity, in contrast with previous reports. The apparent specificity of HGO for HGA was highest at pH 6.2 and the steady-state cleavage of HGA fit a compulsory-order ternary-complex mechanism (K_m value of 28.6 ± 6.2 μM for HGA, K_m value of 1240 ± 160 μM for O_2). Free HGO was subject to inactivation in the presence of O_2 and during the steady-state cleavage of HGA. Both cases involved the oxidation of the active site Fe(II). 3-Cl HGA, a potential inhibitor of HGO, and its isosteric analogue, 3-Me HGO, were synthesized. At saturating substrate concentrations, HGO cleaved 3-Me and 3-Cl HGA 10 and 100 times slower than HGA respectively. The apparent specificity of HGO for HGA was approx. two orders of magnitude higher than for either 3-Me or 3-Cl HGA. Interestingly, 3-Cl HGA inactivated HGO only twice as rapidly as HGA. This contrasts with what has been observed in mechanistically related dioxygenases, which are rapidly inactivated by chlorinated substrate analogues, such as 3-hydroxyanthranilate dioxygenase by 4-Cl 3-hydroxyanthranilate.

Key words: alkaptonuria, dioxygenase, enzymology, homogentisate, inhibition, tyrosine catabolism.

INTRODUCTION

Just over 100 years ago, Garrod discovered that alkaptonuria is caused by a defect in a single gene [1]. This discovery provided the first evidence that an inherited defect causes an inborn error of metabolism, and essentially founded the field of biochemical genetics. The defective enzymic activity was finally characterized in 1950 [2], but was not linked to the disease until 1958 [3]. The enzyme, HGO (homogentisate 1,2-dioxygenase; EC 1.13.11.5), is Fe(II)-dependent [2] and utilizes dioxygen (O_2) to catalyse the cleavage of HGA (homogentisate; 2,5-dihydroxyphenylacetate) between C-1 and C-2 of the aromatic ring to yield maleylacetoacetate (Scheme 1 [4]). HGO occurs in the catabolism of phenylalanine and tyrosine and its defect causes the accumulation of large quantities of HGA in the urine that darkens on exposure to air, a key characteristic of alkaptonuria. The accumulation of HGA in several tissues gives rise to pigmentation (ochronosis) and, eventually, serious arthropathy [5,6].

Human HGO is a hexameric enzyme (α_6) with a subunit molecular mass of approx. 50 kDa [7]. The enzyme possesses the structural fold of a cupin [7], a functionally diverse superfamily [8] that includes GO (gentisate 1,2-dioxygenases; EC 1.13.11.4). GO, a bacterial enzyme, catalyses the same mode of cleavage as HGO. The crystal structure of HGO reveals further that the active site Fe(II) is co-ordinated by two histidine residues and a glutamate. This 2-His-1-carboxylate facial triad is found in many mononuclear iron enzymes [9], including extradiol dioxygenases. GO and extradiol dioxygenases are involved in the microbial catabolism of a wide range of aromatic compounds [10]. The similarity between the environment of the active site Fe(II) of GO and the better characterized extradiol dioxygenases had initially been suggested by EPR spectroscopic studies [11,12].

Although HGO has been studied for over 50 years, many aspects of the reactivity of this enzyme are unclear. For example, most studies have relied on the addition of ferrous iron and reducing agents to prevent oxidation of the active site iron and to achieve maximal enzymic activity [13–24]. Moreover, kinetic characterization of mammalian HGOs have yielded very different results, with reported K_m values for HGA ranging from 6.2 μM for human HGO [19] to 188 μM for murine HGO [21]. As these enzymes share 93 % sequence identity, it is unclear whether these parameters reflect differences between the enzymes or differences in sample preparation. Similarly, kinetic characterization of the enzyme with its second substrate, O_2, has yielded different results, with reported K_m values ranging from 99 μM to 1 mM for human and calf HGO respectively [14,17,25].

A mechanism for the cleavage of HGA by HGO can be proposed based on spectroscopic, structural and kinetic studies of the

Abbreviations used: C23O, catechol 2,3-dioxygenase; DHB, 2,3-dihydroxybiphenyl; DHBD, 2,3-dihydroxybiphenyl 1,2-dioxygenase; DTT, dithiothreitol; GO, gentisate 1,2-dioxygenase; HAD, 3-hydroxyanthranilate dioxygenase; HGA, homogentisate; HGO, homogentisate 1,2-dioxygenase.

[1] These authors have contributed equally to this work.

[2] Present address: Department of Public Health and Food Science, Faculty of Veterinary Medicine, Utrecht University, NL-3508 TD Utrecht, The Netherlands.

[3] Present address: Department of Biological Chemistry and Molecular Pharmacology, Harvard Medical School, 240 Longwood Ave, Boston, MA 02115, U.S.A.

[4] To whom correspondence should be addressed (email leltis@interchange.ubc.ca).

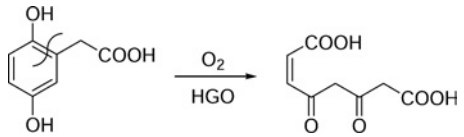

Scheme 1 Reaction catalysed by HGO

mechanistically related extradiol dioxygenases [26–31] and EPR studies of GO [11,12]. Accordingly, HGA first binds to the active site Fe(II) through the carboxylate and the hydroxyl ion at C-2, activating the Fe(II) towards O_2 binding. On O_2 binding, Fe(II) mediates electron transfer from HGA to O_2, yielding a semiquinone-like-Fe(II)-superoxide intermediate, which then reacts to give an iron-alkylperoxo intermediate bridged to C-2. Rearrangement and O–O bond cleavage yields an unsaturated lactone intermediate, which is hydrolysed to yield the reaction product. Few aspects of this proposed catalytic mechanism have been tested.

Extradiol-type dioxygenases can be inhibited or inactivated by halogenated substrate analogues. Thus HAD (3-hydroxyanthranilate dioxygenase) is reversibly inhibited *in vivo* by 4-Cl 3-hydroxyanthranilate and 4,6-diBr 3-hydroxyanthranilate [32,33]. Similarly, DHBD (2,3-dihydroxybiphenyl 2,3-dioxygenase [34]) and C23O (catechol 2,3-dioxygenase [35]) are reversibly inhibited by 3-Cl catechol in a mechanism that involves oxidation of the active site Fe(II). *In vivo* inhibitors of HGO would be useful to model the effects of alkaptonuria on cellular metabolism. They may also assist in the study and improved treatment of hereditary tyrosinemia type I, a disease that often leads to hepatic carcinoma. The disease is caused by a deficiency of fumarylacetoacetate hydrolase [36,37], the last enzyme of the tyrosine pathway.

In the present study, we report the anaerobic purification of a highly active, homogeneous preparation of human HGO. The effect of various additives on this preparation, including reductants and ferrous iron, was investigated. The steady-state cleavage of HGA was investigated as a function of HGA and O_2 concentration, as well as pH and temperature. The lability of the enzyme to O_2 was studied under a similar range of conditions. Finally, the reactivity towards 3-Me HGA, 3-Cl HGA and gentisate was investigated. The described purification method and kinetic analyses provide a basis to investigate this enzyme further.

EXPERIMENTAL

Chemicals

Homogentisic acid (HGA), gentisic acid and Ferene S were from ICN Biomedicals (Costa Mesa, CA, U.S.A.). Factor Xa was purchased from Haematologic Technologies (Essex Junction, VT, U.S.A.). All other chemicals were of analytical grade.

Synthesis of substituted HGAs

3-Me and 3-Cl HGA were synthesized as outlined in Scheme 2. 3-Me-HGA was prepared in four steps from commercially available 2,6-dimethylhydroquinone (**1**, Scheme 2A). Silylation of **1** using an excess of TBSCl (*t*-butyldimethylsilyl chloride) provided compound **2** in excellent yield. Benzylic bromination of **2** using 1 equiv. of NBS (N-bromosuccinimide) in the presence of 1,1′-azobis(cyclohexanecarbonitrile) (ACN [38]) provided an inseparable mixture of the desired bromide **3** with dibromide **4** (9:1 ratio) in 92 % yield. This mixture was treated with sodium cyanide in DMSO to give nitrile **5** in 85 % yield after purification on silica

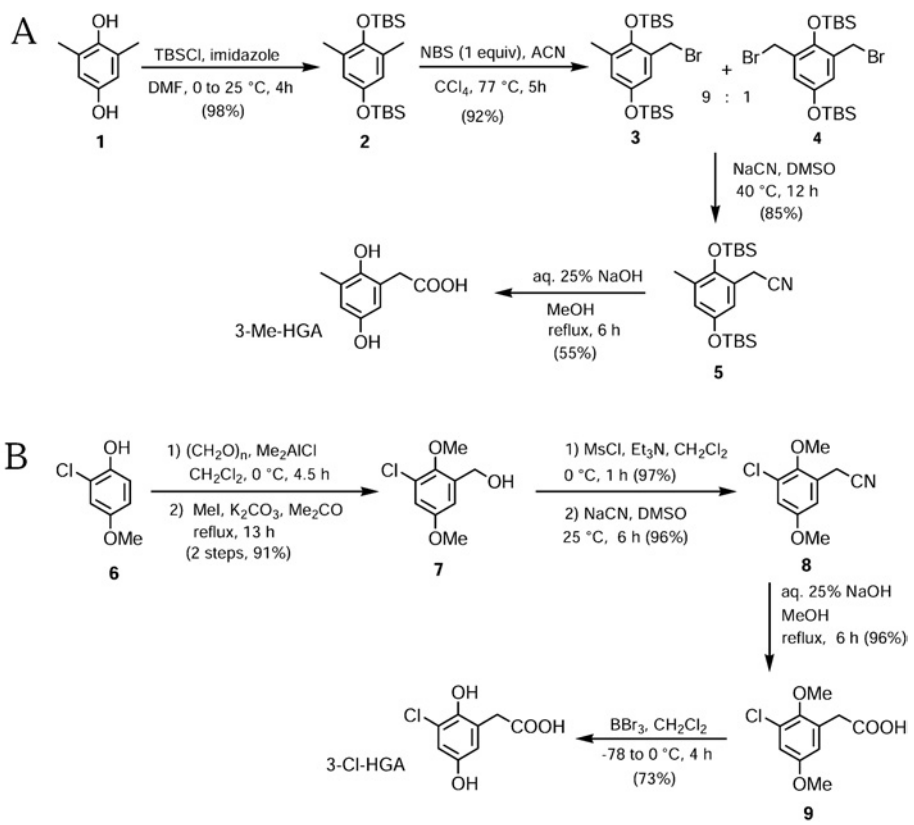

Scheme 2 Synthesis of (A) 3-Me and (B) 3-Cl HGA

gel. Hydrolysis of **5** under basic conditions provided 3-Me HGA in 55 % yield after chromatography as a pale yellow powder [mp 99 °C; ^{1}H NMR (300 MHz, $CDCl_3$) δ 8.05 (s, 1H), 6.54 (s, 2H), 3.59 (s, 2H), 2.17 (s, 3H); ^{13}C NMR (75 MHz, $CDCl_3$) δ 174.6, 151.0, 147.0, 127.0, 123.5, 117.1, 115.7, 37.1, 16.9].

The synthesis of 3-Cl HGA (Scheme 2B) began with regioselective hydroxymethylation of phenol **6** and subsequent methylation of the phenol group to furnish alcohol **7** as described by Kitamura et al. [39]. Mesylation of **7** and subsequent treatment with sodium cyanide in DMSO furnished nitrile **8** with a high overall efficiency. Hydrolysis of **8** provided the corresponding carboxylic acid **9** in 96 % yield. Exposure of **9** to boron tribromide accomplished deprotection of both phenyl groups [40] to give 3-Cl HGA (73 % yield after chromatography) as a pale yellow powder [mp 70–72 °C; ^{1}H NMR (300 MHz, $CDCl_3$) δ 11.50 (s, 1H), 6.88 (d, $J = 2.9$ Hz, 1H), 6.70 (d, $J = 2.9$ Hz, 1H), 3.68 (s, 2H); ^{13}C NMR (75 MHz, $CDCl_3$) δ 172.9, 151.2, 144.8, 125.6, 121.4, 117.8, 115.3, 36.4].

Strains, media and growth

Escherichia coli DH5α was used for DNA propagation and was cultured at 37 °C and 200 rev./min in LB (Luria–Bertani) broth with the appropriate antibiotics. *E. coli* GJ1158 [41] transformed with a pLEPH20 [42] derivative was used for overexpression and was cultured at 37 °C and 200 rev./min in LB medium without NaCl and was supplemented with a potassium phosphate buffer described for Terrific Broth [43], HCl-solubilized ferrous sulphate to a final concentration of 40 μM and 20 μg/ml carbenicillin.

Construction of plasmids and overexpression of protein

DNA was purified, manipulated and transformed according to standard methods [43]. The HGO gene was amplified by PCR from a human liver cDNA bank [44] using two primers: HGOfor (5′-GCGCATATGGCTGAGTTAAAGTACA-3′) that introduces an *Nde*I site (underlined) at the start codon of the HGO gene, and HGOrev (5′-GGGCTGCAGTCTCAATTAGGTTCT-3′) that introduces a *Pst*I site (underlined) after the stop codon of the HGO gene. PCRs were performed using Expand High Fidelity PCR system (Roche Applied Science, Laval, QC, Canada) according to the manufacturer's instructions and the following optimized cycling method: 1 cycle at 95/50/72 °C for 5/5/40 min respectively, 5 cycles at 95/50/72 °C for 40/60/120 s respectively, 25 cycles at 95/65/72 °C for 30/30/120 s respectively and one 10 min incubation at 72 °C. The resulting amplicon was digested and cloned into pT7-7 [45] yielding the expression plasmid pFVHGO-1. The cloned DNA was sequenced in both orientations using an ABI 373 Stretch (Applied Biosystems, Foster City, CA, U.S.A.) and Big-Dye terminators to confirm that it contained no errors. To facilitate purification of the recombinant enzyme, a His tag was introduced at the N-terminal of the protein. The HGO gene was amplified from pFVHGO-1 using the same PCR system, the standard M13 forward primer (Stratagene, La Jolla, CA, U.S.A.) and HGOfor2 (5′-TATCTAGCTAGCATGGCTGAGTTAAAGT-3′) that introduces an *Nhe*I site (underlined) immediately before the starting codon of the HGO gene. The resulting DNA fragment was digested, cloned into pEMBL18 [46] to yield pEDHGO-1, and sequenced again to verify that no errors had been introduced. The insert was then subcloned using *Nhe*I and *Pst*I into pLEPH20 [42] yielding the expression plasmid pEDHGO-2.

His-tagged HGO was overexpressed in *E. coli* GJ1158 [41] transformed with pEDHGO-2. Cultures (1 litre) in 2 litres Erlenmeyer flasks were inoculated with 1 ml of an overnight culture. The cultures were incubated for 16–17 h and then harvested.

Protein purification

All buffers were prepared using water purified on a Barnstead NANOpure UV apparatus to a resistivity of > 17 M$\Omega \cdot$ cm. Unless otherwise specified, all cell-free preparations of HGO were manipulated under an inert atmosphere using an Mbraun Labmaster glovebox (Stratham, NH, U.S.A.) maintained at 2 p.p.m. O_2 or less. Chromatography was performed using an ÄKTA Explorer 100 (Amersham Biosciences, Montreal, QC, Canada) configured to maintain an anaerobic atmosphere during purification, as described previously [47]. Buffers were sparged with N_2 and equilibrated in the glovebox for at least 24 h before use.

A cell pellet from 6 litres of culture was resuspended in buffer A (20 mM Hepps, pH 8.0, 300 mM NaCl). The cells were disrupted by two successive passages through a French press operated at 12 500 psi and 4 °C. The cell debris was removed by ultracentrifugation at 100 000 ***g*** for 60 min in gas-tight tubes. The supernatant was carefully removed. This 'raw extract' was incubated with 40 ml of Ni^{2+}-nitrilotriacetate superflow resin (Qiagen, Mississauga, ON, Canada) for 2 h and poured in a low-pressure chromatography column (2.5 cm diameter; Bio-Rad, Mississauga, ON, Canada). The resin was washed successively with three column volumes of buffer A and four column volumes of buffer A containing 20 mM imidazole to remove unbound and non-specifically bound contaminants respectively. HGO was eluted using buffer A containing 250 mM imidazole. The eluate was immediately applied to a size exclusion chromatography column (Bio-Rad P6-DG) equilibrated with buffer B (20 mM Hepps, pH 8.0, 100 mM NaCl) to remove imidazole and lower the NaCl concentration. The eluate was adjusted to 2 mM $CaCl_2$, and the solution of HGO was incubated for 3 h at room temperature with Factor Xa (FXa/HGO, 1:500, w/w) to remove the His tag. HGO was then exchanged into buffer C [20 mM Tris, pH 8.7, 10 % (v/v) glycerol] using an Amicon stirred cell concentrator (Millipore Canada, Nepean, ON, Canada) and the solution was divided into four equal portions. Each portion was loaded on to a MonoQ anion exchange HR 16/10 column (Amersham Biosciences) equilibrated with buffer C. HGO was eluted using a NaCl gradient of 0–250 mM over 10 column volumes at a flow rate of 5 ml/min. Fractions of 4 ml were collected and checked for activity using a colorimetric assay (see below). HGO eluted at approx. 90 mM NaCl and purity was verified by SDS/PAGE [43]. The fractions with the highest specific activity were pooled, exchanged into buffer D (20 mM Hepps, pH 8.0, 100 mM NaCl), concentrated to 3–5 mg/ml, flash frozen in liquid nitrogen and stored in 50–100 μl aliquots at -80 °C until further use. No significant loss of activity was observed over a period of 4 months.

MS analysis

The molecular mass of His-tagged and cleaved HGO was evaluated by ionspray MS as described previously [34].

Handling of HGO samples

Aliquots of HGO were anaerobically thawed immediately before use and diluted further in buffer D containing 10 % glycerol. Dilutions of HGO were removed from the glovebox, placed under argon and stored on ice.

SDS/PAGE was performed in a Bio-Rad MiniPROTEAN II apparatus and stained with Coomassie Blue according to established procedures [43]. Protein concentrations were determined

by the Bradford method [48]. Iron concentrations were determined colorimetrically using Ferene S [49].

HGO activity assays

The steady-state cleavage of HGA by HGO was generally monitored using an oxygen electrode assay. The assay was performed in a total volume of 1.4 ml of air-saturated 20 mM Mes, 80 mM NaCl ($I = 0.1$), pH 6.2 at 25 °C containing 100 μM HGA. The reaction was initiated by injecting an appropriate amount of HGO into the reaction chamber, and the consumption of O_2 was monitored using a calibrated Clark-type polarographic electrode (Yellow Springs Instruments Model 5301, Yellow Springs, OH, U.S.A.) as described previously [47]. Data were recorded every 0.1 s and initial velocities were calculated from the slope of the progress curve for each consecutive 6 s interval. In each assay, the substrate concentration and reaction velocities were monitored for 10–20 s after the initiation of the reaction and compared with calculated values to evaluate the degree of inactivation of the enzyme during the reaction [47]. Assays in which > 15 % inactivation occurred were discarded. One unit of enzymic activity was defined as the quantity of enzyme that consumed 1 μmol of O_2 per min. Concentrations of active HGO in the assay were defined by the iron content of the injected purified enzyme solution and were used in calculating specificity, catalytic and inactivation constants.

A more convenient spectrophotometric assay [16] was used to monitor HGO activity during purification and sample handling, as well as for certain experiments. The assay contained 1 ml of buffer and 100 μM HGA, and the production of maleylacetoacetate was monitored at 330 nm [$\varepsilon = 10.1\ mM^{-1} \cdot cm^{-1}$, 20 mM Mes, 80 mM NaCl ($I = 0.1$), pH 6.2, 25 °C].

Dependence of HGO activity on pH and additives

The pH dependence of HGO activity was determined over the range from 5.0 to 8.0 at 25 °C using the following Good buffers: Mes (pH 5.0–6.5), Mops (pH 6.75, 7.0), Hepes (pH 7.5) and Hepps (pH 8.0) [20 mM buffer, 80 mM NaCl ($I = 0.1$)]. The activity of HGO at some of these pH values was also tested using potassium phosphate buffers. The effect of each of the following reducing agents on the activity of HGO was tested in the presence and absence of 0.25 mM $Fe(NH_4)_2SO_4 \cdot 6H_2O$ using the standard assay: 2 mM DTT (dithiothreitol), 2 mM GSH and 2 mM ascorbate. The effect of 5 mM EDTA on the activity of HGO was also tested.

Stability of HGO activity

The stability of HGO activity in aerobic buffer was studied by incubating HGO in the oxygen electrode cuvette for different periods of time t and determining the remaining activity A_t by adding 100 μM HGA to the cuvette. The apparent first-order rate constant of inactivation j_1^{app} was determined from A_t and t as described previously (see eqn 1 of [34]). Stability was studied in Mes (pH 5.5 and 6.2), Mops (pH 7.0) and in Hepps (pH 8.0); [20 mM buffer, 80 mM NaCl ($I = 0.1$)]. It was also evaluated in potassium phosphate buffer ($I = 0.1$), at similar pH values.

Coupling of the reaction

The coupling of HGA and O_2 consumption was investigated by monitoring the amount of O_2 consumed on the addition of weighed amounts of HGA to the reaction mixture and an excess of HGO. The O_2 electrode was calibrated using standard concentrations of DHBD and DHB (2,3-dihydroxybiphenyl), a well coupled system [47].

Specificity experiments

All substrate solutions and aerobic buffers were prepared fresh daily. HGA and gentisate were sufficiently stable in aerobic buffers and they were dissolved in water and stored aerobically on ice. 3-Me and 3-Cl HGAs were dissolved anaerobically in 20 mM Mes, 80 mM NaCl ($I = 0.1$), pH 6.2, and were stored under argon and on ice when removed from the glovebox. Appropriate steady-state equations were fit to initial velocity data using the least squares and dynamic weighting options of LEONORA [50].

The steady-state cleavage of HGA and 3-Me HGA were studied using the oxygen electrode assay. The concentrations of these compounds were varied from 5 to 120–150 μM and 25 to 650 μM respectively. To determine the apparent specificity of HGO for O_2 in the presence of 250 μM HGA, the concentration of O_2 was varied from 25 to 1300 μM.

To investigate the steady-state mechanism of HGO, the concentrations of HGA and O_2 were varied from 5 to 300 μM and from 25 to 1300 μM respectively. Different rate equations were fit to the data, including one describing a compulsory order ternary complex mechanism (eqn 1).

$$v = \frac{V[A][O_2]}{K_{dA}K_{mO2} + K_{mA}[O_2] + K_{mO2}[A] + [A][O_2]} \quad (1)$$

In this equation, v and V are the initial and the maximal velocity respectively, K_{mA} represents the Michaelis–Menten constant for HGA, K_{mO2} the Michaelis–Menten constant for O_2 and K_{dA} the dissociation constant for HGA. An equation describing a substituted (ping-pong) enzyme mechanism was also used (eqn 1 without the $K_{dA}K_{mO2}$ term).

The steady-state cleavage of 3-Cl HGA could only be monitored directly using the more sensitive spectrophotometric assay [at 330 nm, $\varepsilon = 12.0\ mM^{-1} \cdot cm^{-1}$; 20 mM Mes, 80 mM NaCl ($I = 0.1$), pH 6.2]. The concentrations of 3-Cl HGA were varied from 5 to 500 μM.

The K_{ic}^{app} of HGO for gentisate was determined using HGA as a reporter substrate in the oxygen electrode assay. The concentration of gentisate was varied from 0.25 to 2.5 mM and the concentration of HGA was varied from 10 to 120 μM. The competitive inhibition equation was fit to the data [50].

Mechanism-based inactivation studies

In experiments designed to determine the partition ratio for HGA or 3-Me HGA, the concentration of these compounds was 300 μM in air-saturated buffer. The amount of HGO was chosen such that the enzyme was completely inactivated before more than 15 % of any substrate was consumed. The partition ratio was calculated by dividing the amount of O_2 consumed by the amount of active HGO added to the assay (see eqn 2 of [34]).

For HGA or 3-Me HGA, the apparent rate constant of inactivation during catalytic turnover in air-saturated buffer, termed j_3^{app} [34], was calculated from the partition ratio determined under saturating substrate conditions ($[S] \gg K_m$). Under such conditions, the concentration of free enzyme [E] is negligible, and the partition ratio is equal to the ratio of the catalytic constant k_{cat}^{app} and the inactivation constant j_3^{app} (see eqn 2 of [34]).

For 3-Cl HGA, j_3^{app} was determined from progress curves at 330 nm (see eqns 3 and 4 of [34]) recorded in the presence of 1 mM 3-Cl HGA. The j_3^{app} value for gentisate was estimated using HGA as a reporter substrate (see eqns 3 and 5 of [34]). The appearance of maleylacetoacetate was monitored at 330 nm in air-saturated 20 mM Mes, 80 mM NaCl ($I = 0.1$), pH 6.2. The concentrations of HGA and gentisate were 300 and 500 μM respectively. The concentration of gentisate could not be increased

above 500 μM due to the high absorbance of this compound ($\lambda_{max} = 320$ nm, $\varepsilon = 4.3$ $mM^{-1} \cdot cm^{-1}$ and $\varepsilon = 3.6$ $mM^{-1} \cdot cm^{-1}$ at $\lambda = 330$ nm).

In vitro inactivation and reactivation of HGO

HGO was inactivated *in vitro* using two different methods, each performed at 23 °C using 20 mM Mes, 80 mM NaCl, ($I = 0.1$), pH 6.2. In the first experiment, HGO was inactivated anaerobically by incubating a 30 μM solution of the protein with 5 mM 1,10-phenanthroline for 10 min. In the second experiment, HGO was inactivated by incubating a 30 μM solution of the enzyme with 8 mM 3-Cl HGA. In this experiment, the reaction mixture was maintained under a gentle stream of O_2 for 10 min. The activity of the preparations was monitored using the standard assay to verify inactivation. Attempts to reactivate inactivated samples of HGO, in 20 mM Mes, 80 mM NaCl, ($I = 0.1$), pH 6.2, were performed in a glovebox as described for DHBD [34].

In vivo inhibition of HGO

Assays were performed using *E. coli* GJ1158 transformed with pEDHGO-2. Cells were grown for 16–17 h, harvested by centrifugation, and washed twice with potassium phosphate buffer (pH 7.0, $I = 0.1$) containing 100 μg/ml chloramphenicol to prevent protein synthesis. The activity of HGO was followed using a modification of the oxygen electrode assay as described above. In the non-inhibited assay, whole cells were injected into a reaction mixture containing potassium phosphate buffer, pH 7.0 ($I = 0.1$), 100 μg/ml chloramphenicol followed by the addition of 500 μM HGA. In the inhibited assay, whole cells were added to the same buffer as above and 1 mM 3-Cl HGA was added followed by a 5 min incubation after which 500 μM HGA was added to determine the remaining activity.

RESULTS

Purification

Of the expression systems tested, highest yields of recombinant human HGO were obtained from *E. coli* GJ1158 transformed with pEDHGO-2. The strain contains an NaCl-inducible T7 polymerase and the plasmid contains the HGO gene under control of P_{lac}. The addition of neither NaCl nor isopropyl β-D-thiogalactopyranoside increased the expression of the recombinant protein. HGO was purified anaerobically to apparent homogeneity using IMAC (immobilized metal affinity chromatography) and anion exchange chromatography. The His tag was completely cleaved after a 3 h incubation with Factor Xa. Cleavage was detected as a small band shift on SDS/PAGE (results not shown). The molecular masses of His-tagged and cleaved HGO were 51 690 and 50 150 respectively, as determined by MS. These values are in good agreement with the predicted masses of 51 799.77 and 50 130.96 Da respectively.

Relevant details of the purification are shown in Table 1. A total of 48.5 mg of HGO was obtained from 6 litres of cell culture and a 2.6-fold increase in specific activity was observed on purification. The iron content of purified HGO was typically 50–55 % using this procedure. In contrast, the iron content of the His-tagged protein was generally close to 100 %. Nevertheless, the specific activity of the His-tagged HGO (based on iron content) was always lower than that of the cleaved protein. This suggests that the His tag affected the catalytic activity of HGO or that not all of the iron was present at the active site. Accordingly, the cleaved protein was used in all experiments described in the present study.

Table 1 Purification details of human HGO expressed in *E. coli* GJ1158

Activity units were measured at 25 °C and are defined in the Experimental section.

Purification step	Total protein (mg)	Total activity (units)	Specific activity (units/mg)	Yield (%)
Raw extract	1800	19260	10.7	100
Ni-affinity	167	3841	23.0	19.9
Mono Q	48.5	1374	28.3	7.1

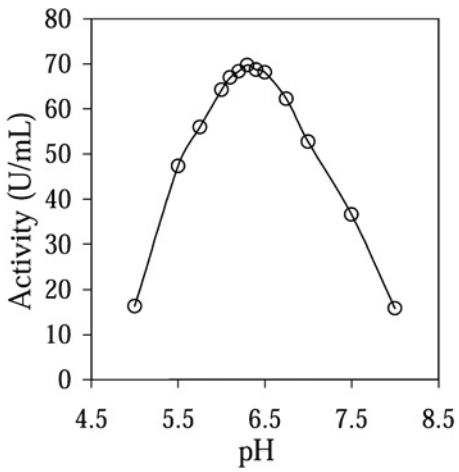

Figure 1 pH dependence of the activity of HGO

The pH of the assay buffer was varied between 5.0 and 8.0 using 20 mM Good buffer, 80 mM NaCl ($I = 0.1$): Mes (pH 5.0–6.5), Mops (pH 6.75, 7.0), Hepes (pH 7.5) and Hepps (pH 8.0). All experiments were performed at least in duplicates using 100 μM HGA at 25 °C.

Determination of optimal pH and assay optimization

In Good buffers, HGO showed maximal activity at pH 6.2 (Figure 1). Similar results were obtained using potassium phosphate buffers. All tested additives had a deleterious effect on the activity of HGO at this pH. The reduction of activity in the presence of 2 mM ascorbic acid (38 %; pH readjusted to 6.2) was greater than in the presence of either 5 mM EDTA, 2 mM DTT or 2 mM GSH (5–10 % reduction). The addition of 0.25 mM $FeSO_4 \cdot 7H_2O$ resulted in a 42 % decrease in activity. This decrease was not as great when either 2 mM DTT, 2 mM GSH or 2 mM ascorbic acid was added together with the iron ($\sim$ 10–20 % reduction). Accordingly, the standard assay was performed at pH 6.2 in the absence of additives.

Stability in the presence of O_2 and coupling of the reaction

The stability of HGO activity in air-saturated buffer at 25 °C was pH-dependent. In Good buffers, the pseudo-first-order rate constant of inactivation of HGO, j_1^{app}, was lowest at the basic end of the tested pH range (pH 8; Table 2), corresponding to a half-life of 16.5 ± 0.9 min. The half-life of enzyme activity was approx. 4-fold shorter at pH 6.2, where the enzyme was most active. Moreover, the half-life of the enzyme was two to ten times longer in Good buffers versus potassium phosphate buffer at the same pH values and ionic strength ($I = 0.1$). Accordingly, only Good buffers were used in the further characterization of purified HGO. At 37 °C, the half-life of HGO was 28 ± 3 and 17 ± 3 s at pH 6.2 [20 mM Mes, 80 mM NaCl ($I = 0.1$)] and pH 7.0 [20 mM Mops, 80 mM NaCl ($I = 0.1$)] respectively.

Table 2 Apparent steady-state kinetic parameters and inactivation parameters of recombinant HGO from human liver for HGA at different pH values and temperatures

Values in parentheses represent standard errors. Experiments were performed using air-saturated Mes (pH 6.2 and 5.5), Mops (pH 7.0) and Hepes (pH 8.0); [20 mM buffer, 80 mM NaCl ($I = 0.1$)].

pH	Temperature (°C)	j_1^{app} ($\times 10^{-3}$ s^{-1})	K_{mA}^{app} (μM)	k_{cat}^{app} (s^{-1})	k_A^{app} ($\times 10^6$ M$^{-1}\cdot$s^{-1})	Partition ratio	j_3^{app}* ($\times 10^{-3}\cdot$s^{-1})	j_3^{app}/K_{mA}^{app}† ($\times 10^3$ M$^{-1}\cdot$s^{-1})
5.5	25	12.8 (0.6)	42.0 (3.8)	41.5 (1.7)	0.99 (0.06)	7300 (500)	5.7 (0.6)	0.14 (0.03)
6.2	25	2.6 (0.4)	22.3 (0.9)	56.0 (1.1)	2.51 (0.06)	13700 (700)	4.1 (0.3)	0.18 (0.02)
7.0	25	4.8 (0.4)	16.3 (0.6)	32.2 (0.5)	1.97 (0.05)	7700 (300)	4.2 (0.2)	0.26 (0.02)
8.0	25	0.70 (0.04)	9.1 (0.6)	10.1 (0.2)	1.11 (0.06)	1430 (50)	7.1 (0.4)	0.78 (0.10)
6.2	37	25 (3)	15.0 (0.9)	64.3 (1.3)	4.3 (0.2)	5150 (240)	12.5 (0.8)	0.83 (0.10)
7.0	37	40 (6)	13.5 (0.6)	43.4 (0.5)	3.2 (0.1)	1330 (50)	32.6 (1.6)	2.4 (0.2)

* Values calculated by dividing the k_{cat}^{app} by the partition ratio to obtain j_3^{app} (see eqn 2 of [34]).

† Values calculated by dividing the calculated j_3^{app} by K_{mA}^{app} to obtain j_3^{app}/K_{mA}^{app}.

Under standard assay conditions, the amount of O_2 consumed corresponded to the amount of HGA added to the reaction mixture, indicating that the cleavage of HGA by HGO was tightly coupled with the consumption of O_2. The same was shown for 3-Me HGA and O_2 utilization. In subsequent experiments, the O_2 electrode was sometimes calibrated with HGO and HGA instead of DHB and DHBD.

Steady-state kinetic analysis

In air-saturated buffer using HGA as a substrate, the k_{cat}^{app} and specificity constant k_A^{app} followed the same trend over pH 5.5 to pH 8.0 as the pH curve described in Figure 1, both were optimal at pH 6.2. However, as the pH increased, the K_{mA}^{app} values decreased. Examples of the data and the quality of the fit are shown in Figure 2(A). At higher substrate concentrations (500–2000 μM), minor substrate inhibition was observed at all pH values ($K_{iA}^{app} \sim 10$ mM).

The partition ratio of HGO for HGA was highest at pH 6.2 and also followed the same trend as the pH curve depicted in Figure 1. This reflects not only the k_{cat}^{app} value, which is optimal at pH 6.2, but also the j_3^{app} value, which is lowest at pH 6.2 (partition ratio = k_{cat}^{app}/j_3^{app}). Consideration of the j_3^{app}/K_{mA}^{app} values indicates that HGO is increasingly susceptible to inactivation as pH is increased from 5.5 to 8.0.

At 37 °C, a more physiological temperature, the k_{cat}^{app} of HGO, was approx. 1.2-fold higher than at 25 °C, and the apparent specificity constant for HGA was approx. 1.7-fold higher (Table 2). Similar results were obtained at pH 6.2 and 7.0. However, the enzyme was more susceptible to inactivation at the higher temperature, reflected in the 3- to 6-fold lower partition ratios at pH 6.2 and 7.0 respectively (Table 2). Indeed, at 37 °C, HGO was 4.6 and 9.2 times more susceptible (j_3^{app}/K_{mA}^{app} ratio) to inactivation during catalysis at pH 6.2 and 7.0 respectively when compared with the values obtained at 25 °C. Due to the higher specificity and lower susceptibility to inactivation at pH 6.2, further studies were performed at pH 6.2 and 25 °C.

Under the standard assay conditions, the apparent specificity of HGO for HGA was 60 and 104 times higher than for 3-Me and 3-Cl HGAs respectively (Table 3, Figure 3). However, the k_{cat}^{app} value was 10 times lower for 3-Me HGA and 100 times lower for 3-Cl HGA when compared with the value obtained with HGA. Interestingly, the rate of inactivation during catalysis j_3^{app} for 3-Me and 3-Cl HGAs was less than twice that for HGA. Nevertheless, the partition ratio of HGO was much lower for 3-Cl HGA (Table 3) due to the much smaller k_{cat}^{app} value.

Under standard assay conditions, HGO did not detectably cleave gentisate (the oxygen electrode assay and spectrophotometric assay had respective limits of detection ~ 1 and ~ 0.01 s^{-1}). To investigate further the steady-state utilization of this substrate by HGO, oxygen electrode studies were performed using HGA as a reporter substrate. Under these conditions, the K_{ic}^{app} of HGO for gentisate was 600 ± 100 μM, which is 27 times larger than the K_{mA}^{app} value for HGA. To evaluate j_3^{app}, a spectrophotometric assay was performed using HGA as a reporter substrate. The highest concentration of gentisate that could be used was 500 μM as higher concentrations interfered with the signal at 330 nm. However, no increase in the observed inactivation rate j_s was

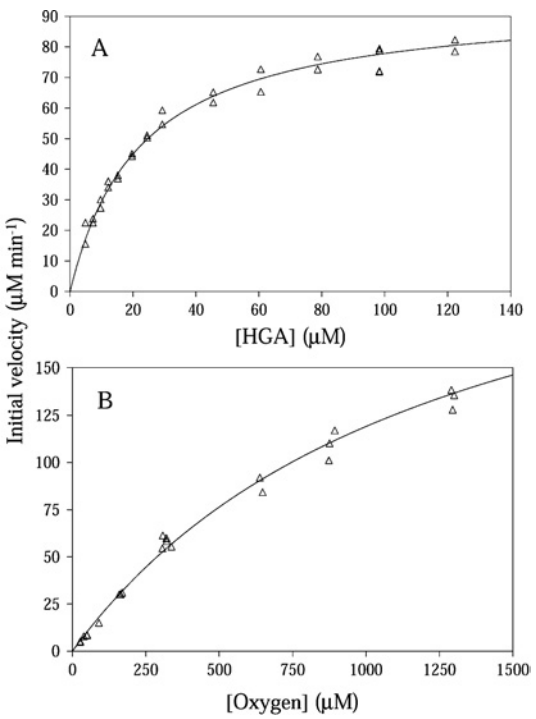

Figure 2 Steady-state cleavage of HGA by recombinant human HGO

(**A**) The dependence of the initial velocity on the concentration of HGA in air-saturated buffer. The line represents a best fit of the Michaelis–Menten equation to the data. The fit parameters are $K_{mA}^{app} = 22.3 \pm 0.9$ μM and $V = 95.2 \pm 1.8$ μM/min. (**B**) The dependence of the initial velocity on the concentration of dioxygen using 250 μM HGA. The line represents a best fit of the data to the Michaelis–Menten equation. The fit parameters are $K_{m02}^{app} = 1270 \pm 130$ μM and $V = 270 \pm 19$ μM/min. Initial velocities obtained on different days were normalized according to the amount of enzyme used in the assay. All experiments were performed using 20 mM Mes, pH 6.2, 80 mM NaCl ($I = 0.1$) at 25 °C. Data were fit using the method of least squares, dynamic weighting options of LEONORA.

Table 3 Apparent steady-state kinetic parameters and inactivation parameters of recombinant human HGO for different substrates

Values in parentheses represent standard errors. Experiments were performed using air-saturated 20 mM Mes, 80 mM NaCl ($I = 0.1$), pH 6.2, at 25 °C.

Substrate	K_{mA}^{app} (μM)	k_{cat}^{app} (s^{-1})	k_{A}^{app} ($\times 10^6$ $M^{-1} \cdot s^{-1}$)	Partition ratio	j_3^{app} ($\times 10^{-3} \cdot s^{-1}$)	j_3^{app}/K_{mA}^{app}* ($\times 10^3$ $M^{-1} \cdot s^{-1}$)
HGA†	22.3 (0.9)	56.0 (1.1)	2.51 (0.06)	13700 (700)	4.1 (0.3)‡	0.18 (0.02)
3-Me HGA	127.3 (6.6)	5.3 (0.1)	0.042 (0.002)	720 (20)	7.4 (0.3)‡	0.058 (0.005)
3-Cl HGA	22.1 (1.2)	0.53 (0.01)	0.0241 (0.001)	79 (9)	6.7 (0.6)§	0.31 (0.04)
Gentisate	600 (110)‖					

* Value calculated by dividing j_3^{app} by K_{mA}^{app} to obtain j_3^{app}/K_{mA}^{app}.
† Values are taken from Table 1.
‡ Values are calculated by dividing k_{cat}^{app} by the partition ratio to obtain j_3^{app} (see eqn 2 of [34]).
§ Values are obtained using the spectrophotometric assay for the detection of the cleaved product of 3-Cl HGA (see eqns 3 and 4 of [34]).
‖ Value corresponds to the apparent competitive inhibition constant K_{ic}^{app} obtained using HGA as a reporter substrate in the oxygen electrode assay.

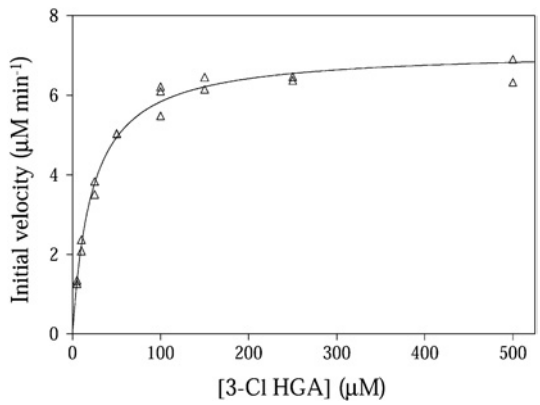

Figure 3 Steady-state cleavage of 3-Cl HGA by recombinant human HGO

The dependence of the initial velocity on the concentration of 3-Cl HGA in air-saturated 20 mM Mes, pH 6.2, 80 mM NaCl ($I = 0.1$) at 25 °C. The line represents a best fit of the Michaelis–Menten equation to the data. The fit parameters are $K_{mA}^{app} = 22.1 \pm 1.2$ μM and $V = 7.1 \pm 0.1$ μM/min. Data were fit using the method of least squares, dynamic weighting options of LEONORA.

observed in the presence of gentisate. Considering its relatively high concentration (500 μM), it is unlikely that gentisate is a strong inactivator of HGO.

To discriminate which steady-state mechanism is utilized by HGO, equations were fit to 139 initial velocity data points obtained over a range of concentrations of HGA and O_2 at pH 6.2. When the steady-state rate equation describing a compulsory order ternary complex mechanism (eqn 1) was fit to the data, random residuals were observed. The values for the steady-state kinetic parameters obtained from this fit are: $K_{dA} = 20.8 \pm 2.7$ μM, $K_{mA} = 28.6 \pm 6.2$ μM, $K_{mO2} = 1240 \pm 160$ μM, $k_{cat} = 216 \pm 20$ s^{-1}, $k_A = (7.6 \pm 1.1) \times 10^6$ $M^{-1} \cdot s^{-1}$ (specificity constant for HGA) and $k_B = (0.175 \pm 0.008) \times 10^6$ $M^{-1} \cdot s^{-1}$ (specificity constant for O_2). Examples of the data and the quality of the fit are shown in Figure 2. When the rate equation describing a substituted (ping-pong) enzyme mechanism (eqn 1 without the $K_{dA}K_{mO2}$ term) was fit to the data, larger residuals were observed and the errors of the calculated parameters were at least twice the values obtained using the compulsory order ternary complex mechanism.

Inactivation-induced changes in HGO

Inactivation-induced changes in HGO were studied in preparations of enzyme inactivated using one of the two different treatments: 1,10-phenanthroline (in the absence of O_2) and 3-Cl HGA (in the presence of O_2). Both treatments resulted in the rapid formation of a white precipitate corresponding to apoprotein. The enzyme could not be reactivated or resolubilized through anaerobic incubation with DTT and/or Fe(II). In the experiment with 1,10-phenanthroline, the characteristic pink colour of the Fe(II)–(1,10-phenanthroline)$_3$ complex was observed. In the experiment with 3-Cl HGA, formation of the white precipitate was only observed on exposure to O_2. This shows that 3-Cl HGA did not remove the active site iron of HGO by chelation. Unfortunately, due to the precipitation of HGO, the molecular mass of the inactivated enzyme could not be determined using MS. These results suggest that removal of the active site iron significantly reduces the solubility of HGO.

Inhibition of HGO *in vivo*

The activity of HGO with HGA in *E. coli* GJ1158 containing pEDHGO-2 was 0.33 unit/A_{600}. Preincubation of the cells with 1 mM 3-Cl HGA for 5 min resulted in a 22 ± 5 % inhibition of the activity.

DISCUSSION

The described rapid anaerobic purification of recombinant human HGO yielded a preparation with a specific activity of 28.3 units/mg at 25 °C in air-saturated buffer. This is more than 50 % higher than that of the most active preparations described to date [19]. The Fe(II) was also shown to be tightly bound to the protein because the iron content of the final preparation was typically 50–55 %, even though no iron was added to the purification buffers. The addition of reducing agents to the assay mixture had no beneficial effect on the activity, suggesting that the iron atom in the active site of the enzyme is in its reduced state. The high specific activity and the absence of activation by reducing agents indicate that the iron ion is tightly bound and maintained in the ferrous state in the active site of the protein during anaerobic purification.

In contrast with our results, many researchers have concluded that HGO has a low affinity for iron [13,17,21–23]. A probable explanation for this apparent discrepancy is that HGO has a much higher affinity for Fe(II) than for Fe(III). More specifically, previous preparations of HGO were aerobic, and probably contained some Fe(III), even in the presence of reducing agents. In such preparations, active site iron would be readily lost as it is oxidized, explaining the observed low affinity for the metal. This was the case in DHBD, a bacterial Fe(II)-containing extradiol dioxygenase [34]. Additional evidence that this occurs in HGO is provided by Tokuyama [23], who showed that the active site iron could be

exchanged with ^{59}Fe under aerobic, but not anaerobic, conditions. Finally, the rate constant of the dissociation of Fe(II) from HGO was recently shown to be very slow under anaerobic conditions (0.00004 s^{-1} [14]).

Other than the k_{cat}, which depends on the Fe(II) content of the enzyme, the steady-state kinetic properties of anaerobically purified human HGO in air-saturated buffers agree fairly well with what has been reported for aerobically purified mammalian enzymes. The pH of maximal activity of anaerobically purified HGO (pH 6.2) is consistent with values of 6.5 and 6.1 reported for bovine [22] and murine HGO [21] respectively. Curiously, an optimal pH of 5.0 was found for HGO from rabbit liver [18]. The apparent K_m values of HGO for HGA in air-saturated buffers are comparable with values reported for aerobically purified enzymes from human (10 μM, pH 7.0 [14]; 6.2 μM, pH 7.4 [19]), rat liver (10.7 μM, pH 6.5 [51]), rabbit liver (10 μM, pH 5.5 [18]) and *Aspergillus nidulans* (9 μM, pH 7 [16]). However, significantly larger values were reported for murine (188 μM, pH 6.0 [21]) and bovine HGOs (400 μM, pH 5.9 [52]). It is unclear whether the reported differences reflect differences in the enzymes, their preparation or experimental design.

The steady-state reactivity of HGO with O_2 is consistent with what has been reported for mechanistically related enzymes, as well as with dioxygenases from the same catabolic pathway. The observed K_{mO2} of HGO, 1240 μM, is well above the concentration of O_2 in air-saturated buffer ($\sim$290 μM) and consistent with the K_{mO2} of 1 mM estimated for an aerobic preparation of calf HGO [17]. In contrast, the K_{mO2} of HGO was reported to be 99 μM in a recent study [14]. However, in this study, DTT and Fe(II) were in the assay buffer, two reagents which react with O_2 in solution [53,54]. The K_{mO2} of GOs from *Pseudomonas testosteroni* and *P. acidovorans* were approximately an order of magnitude lower (55–96 μM [11]). This variation between enzymes is precedented: the K_{mO2} of extradiol dioxygenases varies from 0.7 μM for C23O from *P. pickettii* PKO1 [55] to 1280 μM for DHBD of *Burkholderia* sp. LB400 [47]. The latter value is of the same order of magnitude as the K_{mO2} for HGO. Interestingly, the enzyme catalysing the step preceding HGO in tyrosine/phenylalanine catabolism, human 4-hydroxyphenylpyruvate dioxygenase (EC 1.13.11.27) has a K_{mO2} lower than 50 μM [56]. However, the ability of the two enzymes to utilize O_2 appears to be remarkably comparable: k_B for O_2 approx. 4×10^4 $M^{-1} \cdot s^{-1}$ (calculated value from [56]) for 4-hydroxyphenylpyruvate dioxygenase versus 17.5×10^4 $M^{-1} \cdot s^{-1}$ for HGO. It is possible that the high K_m of HGO for O_2 reflects the low affinity of the free enzyme for O_2, which may have evolved as a protective adaptation against oxidative inactivation as proposed for DHBD [34].

The steady-state kinetic data indicate that HGO utilizes a compulsory order ternary complex mechanism in which HGA binds first to the active site followed by O_2. This is in good agreement with kinetic and spectroscopic studies of extradiol dioxygenases [27,29,30], which are supposed to be mechanistically related and in which it has been shown that the free enzyme first binds the organic substrate to form a binary complex before reacting with O_2. The data are also consistent with EPR studies of GO. In these studies, it was shown that the affinity of GO for NO, an O_2 analogue, increased 40-fold when gentisate was bound to the iron [11,12]. The steady-state mechanism is supported further by a recent study in which the oxidation of HGO in the absence of substrate was shown to be second order and significantly slower than turnover [14]. As noted by the researchers of that study, the reactivity of HGO towards O_2 must therefore increase in the presence of HGA to support the turnover number.

HGO is typical of extradiol-type dioxygenases in that it is susceptible to inactivation during catalytic turnover [47]. More particularly, the inactivation of HGO did not occur through chelation of the active site Fe(II) by its substrates and is O_2-dependent. In analogy to what occurs in DHBD, it is probable that the inactivation occurs through the oxidation of the active site Fe(II) to Fe(III) [34]. The rate of inactivation in the absence of substrate j_1^{app} is of the same order of magnitude as the one in the presence of HGA j_3^{app}. The recently reported rate constant of oxidation of HGO at 4 °C [14] corresponds to a j_1^{app} that is approx. 100-fold higher than that reported in this paper at 25 °C. Notwithstanding the different methods of determining j_1^{app} in the two studies (following the formation of ferric iron by stopped-flow versus following the loss of ring-cleavage activity) and that the composition of the buffer used in the previous study is unclear, it seems probable that the large difference in rate constants reflects differences in the preparations of HGO. In DHBD, the apparent rate constant of inactivation in the absence of substrate is significantly lower than that in the presence of catecholic substrates [34]. This higher reactivity of HGO with O_2 in the absence of substrate may correspond to a smaller activation barrier for the oxidation of the ferrous active site to a ferric species and superoxide when compared with DHBD [57].

It has been proposed that HGO and GO bind their aromatic substrates in a bidentate manner through the carboxylate and the 2-hydroxyl. Using isotopically labelled gentisate, Harpel and Lipscomb [11,12] demonstrated that the carboxylate and 2-hydroxyl, but not the 5-hydroxyl substituent, bind directly to the iron. In studies of HGO from *A. nidulans* [16], HGA analogues lacking a 2-hydroxyl substituent were not turned over and were poor inhibitors of HGA cleavage. The relatively weak interaction of gentisate with HGO ($K_i = 0.6$ mM), and the similarly weak interaction of HGA with GO ($K_i = 2.8$ mM, [11,12]), is consistent with the proposed mode of binding as it suggests that the length of the carboxylate side-chain is an important binding determinant. The 5-hydroxyl substituent and its ability to tautomerize is another important binding determinant [11,12]. From the crystal structure of substrate-free human HGO, it has been proposed that the 5-hydroxyl of HGA forms a hydrogen bond with His-292 [7]. However, the 5-hydroxy group is not an absolute requirement for this mode of ring cleavage as an enzyme with a high GO activity from *Pseudaminobacter salicylatoxidans* BN12 cleaves salicylate [58].

The lower apparent catalytic constants k_{cat}^{app} of HGO for 3-Me and 3-Cl HGAs versus HGA are consistent with what has been reported for C23O and DHBD with 3-Me and 3-Cl catechols as substrates [34,35]. The catalytic constants of two different GOs were also shown to be lower with 3-Me gentisate, 3-Br gentisate and 3-F gentisate when compared with gentisate. The specificity constant was also lower in all cases except with one GO, where the specificity constant was 1.1–1.2 times higher with 3-Me gentisate and 3-Br gentisate [11].

HGO does not appear to be as strongly inhibited by 3-Cl HGA as other extradiol-type dioxygenases are by chlorinated substrate analogues. Thus 3-Cl HGA oxidatively inactivates HGO twice as fast as HGA (j_3^{app}/K_{mA}^{app}). In contrast, 3-Cl catechol oxidatively inactivates DHBD 300 times faster than DHB. Significant differences are also observed in the apparent K_m. Thus the K_{mA}^{app} of HGO for 3-Cl HGA is similar to that for HGA. In contrast, the K_{mA}^{app} of DHBD for 3-Cl catechol (4.8 μM) is less than half that for DHB [34]. Similarly, the K_{ic}^{app} of HAD for 4-Cl 3-hydroxyanthranilate (6 nM [59]) is 180 times lower than the K_{mA}^{app} for 3-hydroxyanthranilate [60]. The relatively poor inhibition of HGO by 3-Cl HGA observed *in vitro* correlates with the *in vivo* data. Thus when cells expressing recombinant HGO were incubated with 1 mM 3-Cl HGA, a 22 ± 5 % inhibition of the HGO activity was observed. In comparison, the *in vivo* activity

of DHBD was completely inhibited when incubated with 400 μM 3-Cl catechol [34] and the *in vivo* activity of HAD was inhibited in a dose-dependent manner by 4-Cl 3-hydroxyanthranilate with an apparent IC_{50} value of 32 μM [33].

Studies on GO and extradiol dioxygenases as well as the structural data that is available for HGO provide valuable insight into the catalytic mechanism of HGO. Nevertheless, many aspects of HGO function have yet to be elucidated. Additional biochemical, spectroscopic and structural data are required to substantiate the occurrence of proposed catalytic intermediates and the roles of conserved active site residues. The described anaerobic preparation of HGO and kinetic characterization with different substrates provides a valuable basis for such studies.

This work was supported in part by a Collaborative Health Research Project from the Natural Sciences and Engineering Research Council of Canada (NSERC) and by the Fonds pour la formation de Chercheurs et l'Aide a la Recherche of Québec (FCAR). F. H. V. was the recipient of Li Tze Fong Memorial and NSERC postgraduate scholarships. We thank J. Poudrier for the human liver cDNA bank and for his technical assistance in cloning the HGO gene, X.-J. Zheng for assisting in the scale-up of the syntheses and S. He for performing the MS analysis.

REFERENCES

1 Garrod, A. E. (1902) The incidence of alkaptonuria: a study in chemical individuality. Lancet **2**, 1616–1620
2 Suda, M. and Takeda, Y. (1950) Metabolism of tyrosine. II. Homogentisicase. J. Biochem. (Tokyo) **37**, 381–385
3 La Du, B. N., Zannoni, V. G., Laster, L. and Seegmiller, J. E. (1958) The nature of the defect in tyrosine metabolism in alcaptonuria. J. Biol. Chem. **230**, 251–260
4 Knox, W. E. and Edwards, S. W. (1955) Homogentisate oxidase of liver. J. Biol. Chem. **216**, 479–487
5 O'Brien, W. M., La Du, B. N. and Bunim, J. J. (1963) Biochemical, pathologic and clinical aspects of alcaptonuria, ochronosis and ochronotic arthropathy. Am. J. Med. **34**, 813–838
6 Phornphutkul, C., Introne, W. J., Perry, M. B., Bernardini, I., Murphey, M. D., Fitzpatrick, D. L., Anderson, P. D., Huizing, M., Anikster, Y., Gerber, L. H. et al. (2002) Natural history of alkaptonuria. N. Engl. J. Med. **347**, 2111–2121
7 Titus, G. P., Mueller, H. A., Burgner, J., Rodriguez de Cordoba, S., Penalva, M. A. and Timm, D. E. (2000) Crystal structure of human homogentisate dioxygenase. Nat. Struct. Biol. **7**, 542–546
8 Dunwell, J. M., Culham, A., Carter, C. E., Sosa-Aguirre, C. R. and Goodenough, P. W. (2001) Evolution of functional diversity in the cupin superfamily. Trends Biochem. Sci. **26**, 740–746
9 Hegg, E. L. and Que, Jr, L. (1997) The 2-His-1-carboxylate facial triad: an emerging structural motif in mononuclear non-heme iron(II) enzymes. Eur. J. Biochem. **250**, 625–629
10 Vaillancourt, F. H., Bolin, J. T. and Eltis, L. D. (2004) Ring-cleavage dioxygenases. In *Pseudomonas* Vol III. Biosynthesis of Macromolecules and Molecular Metabolism (Ramos, J. L., ed.), pp. 359–395, Kluwer Academic/Plenum Publishers, New York
11 Harpel, M. R. and Lipscomb, J. D. (1990) Gentisate 1,2-dioxygenase from *Pseudomonas*. Purification, characterization, and comparison of the enzymes from *Pseudomonas testosteroni* and *Pseudomonas acidovorans*. J. Biol. Chem. **265**, 6301–6311
12 Harpel, M. R. and Lipscomb, J. D. (1990) Gentisate 1,2-dioxygenase from *Pseudomonas*. Substrate coordination to active site Fe^{2+} and mechanism of turnover. J. Biol. Chem. **265**, 22187–22196
13 Adachi, K., Iwayama, Y., Tanokia, H. and Takeda, Y. (1966) Purification and properties of homogentisate oxygenase from *Pseudomonas fluorescens*. Biochim. Biophys. Acta **118**, 88–97
14 Amaya, A. A., Brzezinski, K. T., Farrington, N. and Moran, G. R. (2004) Kinetic analysis of human homogentisate 1,2-dioxygenase. Arch. Biochem. Biophys. **421**, 135–142
15 Crandall, D. I., Krueger, R. C., Anan, F., Yasunobu, K. and Mason, H. S. (1960) Oxygen transfer by the homogentisate oxidase of rat liver. J. Biol. Chem. **235**, 3011–3015
16 Fernandez-Canon, J. M. and Penalva, M. A. (1997) Spectrophotometric determination of homogentisate using *Aspergillus nidulans* homogentisate dioxygenase. Anal. Biochem. **245**, 218–221
17 Flamm, W. G. and Crandall, D. I. (1963) Purification of mammalian homogentisate oxidase and evidence for the existence of ferrous mercaptans in the active center. J. Biol. Chem. **238**, 389–396
18 Hudecova, S., Strakova, Z. and Krizanova, O. (1995) Purification of the homogentisic acid oxidase from mammalian liver. Int. J. Biochem. Cell Biol. **27**, 1357–1363
19 Rodriguez, J. M., Timm, D. E., Titus, G. P., Beltran-Valero de Bernabe, D., Criado, O., Mueller, H. A., Rodriguez de Cordoba, S. and Penalva, M. A. (2000) Structural and functional analysis of mutations in alkaptonuria. Hum. Mol. Genet. **9**, 2341–2350
20 Schepartz, B. (1953) Inhibition and activation of the oxidation of homogentisic acid. J. Biol. Chem. **205**, 185–192
21 Schmidt, S. R., Muller, C. R. and Kress, W. (1995) Murine liver homogentisate 1,2-dioxygenase. Purification to homogeneity and novel biochemical properties. Eur. J. Biochem. **228**, 425–430
22 Takemori, S., Furuya, E., Mihara, K. and Katagiri, M. (1968) Bovine liver homogentisicase: apo and reconstituted holoenzymes. Eur. J. Biochem. **6**, 411–418
23 Tokuyama, K. (1959) Studies on homogentisicase. I. Purification and the role of ferrous ion in the enzymatic action. J. Biochem. (Tokyo) **46**, 1379–1391
24 Tokuyama, K. (1959) Studies on homogentisicase. II. Stoichiometry of the reaction and nature of reactive groups. J. Biochem. (Tokyo) **46**, 1453–1466
25 Crandall, D. I. (1955) Homogentisic acid oxidase. II. Properties of the crude enzyme in rat liver. J. Biol. Chem. **212**, 565–582
26 Arciero, D. M. and Lipscomb, J. D. (1986) Binding of ^{17}O-labeled substrate and inhibitors to protocatechuate 4,5-dioxygenase-nitrosyl complex. Evidence for direct substrate binding to the active site Fe^{2+} of extradiol dioxygenases. J. Biol. Chem. **261**, 2170–2178
27 Arciero, D. M., Orville, A. M. and Lipscomb, J. D. (1985) [^{17}O]Water and nitric oxide binding by protocatechuate 4,5-dioxygenase and catechol 2,3-dioxygenase. Evidence for binding of exogenous ligands to the active site Fe^{2+} of extradiol dioxygenases. J. Biol. Chem. **260**, 14035–14044
28 Hori, K., Hashimoto, T. and Nozaki, M. (1973) Kinetic studies on the reaction mechanism of dioxygenases. J. Biochem. (Tokyo) **74**, 375–384
29 Mabrouk, P. A., Orville, A. M., Lipscomb, J. D. and Solomon, E. I. (1991) Variable-temperature variable-field magnetic circular dichroism studies of the iron(II) active site in metapyrocatechase: implications for the molecular mechanism of extradiol dioxygenases. J. Am. Chem. Soc. **113**, 4053–4061
30 Shu, L., Chiou, Y.-M., Orville, A. M., Miller, M. A., Lipscomb, J. D. and Que, Jr, L. (1995) X-ray absorption spectroscopic studies of the Fe(II) active site of catechol 2,3-dioxygenase. Implications for the extradiol cleavage mechanism. Biochemistry **34**, 6649–6659
31 Vaillancourt, F. H., Barbosa, C. J., Spiro, T. G., Bolin, J. T., Blades, M. W., Turner, R. F. B. and Eltis, L. D. (2002) Definitive evidence for monoanionic binding of 2,3-dihydroxybiphenyl to 2,3-dihydroxybiphenyl 1,2-dioxygenase from UV resonance Raman spectroscopy, UV/Vis absorption spectroscopy, and crystallography. J. Am. Chem. Soc. **124**, 2485–2496
32 Fornstedt-Wallin, B., Lundstrom, J., Fredriksson, G., Schwarcz, R. and Luthman, J. (1999) 3-Hydroxyanthranilic acid accumulation following administration of the 3-hydroxyanthranilic acid 3,4-dioxygenase inhibitor NCR-631. Eur. J. Pharmacol. **386**, 15–24
33 Walsh, J. L., Wu, H.-Q., Ungerstedt, U. and Schwarcz, R. (1994) 4-Chloro-3-hydroxyanthranilate inhibits quinolinate production in the rat hippocampus *in vivo*. Brain Res. Bull. **33**, 513–516
34 Vaillancourt, F. H., Labbé, G., Drouin, N. M., Fortin, P. D. and Eltis, L. D. (2002) The mechanism-based inactivation of 2,3-dihydroxybiphenyl 1,2-dioxygenase by catecholic substrates. J. Biol. Chem. **277**, 2019–2027
35 Wasserfallen, A. (1989) Biochemical and genetical study of the specificity of catechol 2,3-dioxygenase from pseudomonas putida, Ph.D. thesis, University of Geneva
36 Tanguay, R. M., Valet, J. P., Lescault, A., Duband, J. L., Laberge, C., Lettre, F. and Plante, M. (1990) Different molecular basis for fumarylacetoacetate hydrolase deficiency in the two clinical forms of hereditary tyrosinemia (type I). Am. J. Hum. Genet. **47**, 308–316
37 Tanguay, R. M. (2002) Fumarylacetoacetate hydrolase. In Wiley Encyclopedia of Molecular Medicine, pp. 1338–1341, John Wiley & Sons, New York
38 Ryan, T. J., Lecollinet, G., Velasco, T. and Davis, A. P. (2002) Phase transfer of monosaccharides through noncovalent interactions: selective extraction of glucose by a lipophilic cage receptor. Proc. Natl. Acad. Sci. U.S.A. **99**, 4863–4866
39 Kitamura, M., Ohmori, K., Kawase, T. and Suzuki, K. (1999) Total synthesis of pradimicinone, the common aglycon of the pradimicin-benanomicin antibiotics. Angew. Chem. Int. Ed. **38**, 1229–1232
40 Boukouvalas, J., Lachance, N., Ouellet, M. and Trudeau, M. (1998) Facile access to 4-aryl-2(*5H*)-furanones by Suzuki cross coupling: efficient synthesis of rubrolides C and E. Tetrahedron Lett. **39**, 7665–7668
41 Bhandari, P. and Gowrishankar, J. (1997) An *Escherichia coli* host strain useful for efficient overproduction of cloned gene products with NaCl as the inducer. J. Bacteriol. **179**, 4403–4406
42 Eltis, L. D., Iwagami, S. G. and Smith, M. (1994) Hyperexpression of a synthetic gene encoding a high potential iron sulfur protein. Protein Eng. **7**, 1145–1150

43 Ausubel, F. M., Brent, R., Kingston, R. E., Moore, D. D., Seidman, J. G., Smith, H. A. and Struhl, K. (2000) Current Protocols in Molecular Biology, John Wiley & Sons, New York
44 Phaneuf, D., Labelle, Y., Berube, D., Arden, K., Cavenee, W., Gagne, R. and Tanguay, R. M. (1991) Cloning and expression of the cDNA encoding human fumarylacetoacetate hydrolase, the enzyme deficient in hereditary tyrosinemia: assignment of the gene to chromosome 15. Am. J. Hum. Genet. **48**, 525–535
45 Tabor, S. and Richardson, C. C. (1985) A bacteriophage T7 RNA polymerase/promoter system for controlled exclusive expression of specific genes. Proc. Natl. Acad. Sci. U.S.A. **82**, 1074–1078
46 Dente, L. and Cortese, R. (1987) pEMBL: a new family of single-stranded plasmids for sequencing DNA. Methods Enzymol. **155**, 111–118
47 Vaillancourt, F. H., Han, S., Fortin, P. D., Bolin, J. T. and Eltis, L. D. (1998) Molecular basis for the stabilization and inhibition of 2, 3-dihydroxybiphenyl 1,2-dioxygenase by *t*-butanol. J. Biol. Chem. **273**, 34887–34895
48 Bradford, M. M. (1976) A rapid and sensitive method for the quantitation of microgram quantities of protein utilizing the principle of protein-dye binding. Anal. Biochem. **72**, 248–254
49 Haigler, B. E. and Gibson, D. T. (1990) Purification and properties of NADH-ferredoxin$_{NAP}$ reductase, a component of naphthalene dioxygenase from *Pseudomonas* sp. strain NCIB 9816. J. Bacteriol. **172**, 457–464
50 Cornish-Bowden, A. (1995) Analysis of Enzyme Kinetic Data, Oxford University Press, New York
51 Seegmiller, J. E., Zannoni, V. G., Laster, L. and La Du, B. N. (1961) An enzymatic spectrophotometric method for the determination of homogentisic acid in plasma and urine. J. Biol. Chem. **236**, 774–777
52 Tokuyama, K. (1959) Studies on homogentisicase. III. Kinetic studies on the enzyme action. J. Biochem. (Tokyo) **46**, 1559–1568
53 Lambeth, D. O., Ericson, G. R., Yorek, M. A. and Ray, P. D. (1982) Implications for *in vitro* studies of the autoxidation of ferrous ion and the iron-catalyzed autoxidation of dithiothreitol. Biochim. Biophys. Acta **719**, 501–508
54 Netto, L. E. and Stadtman, E. R. (1996) The iron-catalyzed oxidation of dithiothreitol is a biphasic process: hydrogen peroxide is involved in the initiation of a free radical chain of reactions. Arch. Biochem. Biophys. **333**, 233–242
55 Kukor, J. J. and Olsen, R. H. (1996) Catechol 2,3-dioxygenases functional in oxygen-limited (hypoxic) environments. Appl. Environ. Microbiol. **62**, 1728–1740
56 Rundgren, M. (1977) Steady state kinetics of 4-hydroxyphenylpyruvate dioxygenase from human liver (III). J. Biol. Chem. **252**, 5094–5099
57 Davis, M. I., Wasinger, E. C., Decker, A., Pau, M. Y. M., Vaillancourt, F. H., Bolin, J. T., Eltis, L. D., Hedman, B., Hodgson, K. O. and Solomon, E. I. (2003) Spectroscopic and electronic structure studies of 2,3-dihydroxybiphenyl 1,2-dioxygenase: O_2 reactivity of the non-heme ferrous site in extradiol dioxygenases. J. Am. Chem. Soc. **125**, 11214–11227
58 Hintner, J. P., Lechner, C., Riegert, U., Kuhm, A. E., Storm, T., Reemtsma, T. and Stolz, A. (2001) Direct ring fission of salicylate by a salicylate 1,2-dioxygenase activity from *Pseudaminobacter salicylatoxidans*. J. Bacteriol. **183**, 6936–6942
59 Walsh, J. L., Todd, W. P., Carpenter, B. K. and Schwarcz, R. (1991) 4-Halo-3-hydroxyanthranilic acids: potent competitive inhibitors of 3-hydroxy-anthranilic acid oxygenase *in vitro*. Biochem. Pharmacol. **42**, 985–990
60 Schwarcz, R., Okuno, E., White, R. J., Bird, E. D. and Whetsell, Jr, W. O. (1988) 3-Hydroxyanthranilate oxygenase activity is increased in the brains of Huntington disease victims. Proc. Natl. Acad. Sci. U.S.A. **85**, 4079–4081

Received 13 August 2004/22 September 2004; accepted 13 October 2004
Published as BJ Immediate Publication 13 October 2004, DOI 10.1042/BJ20041370